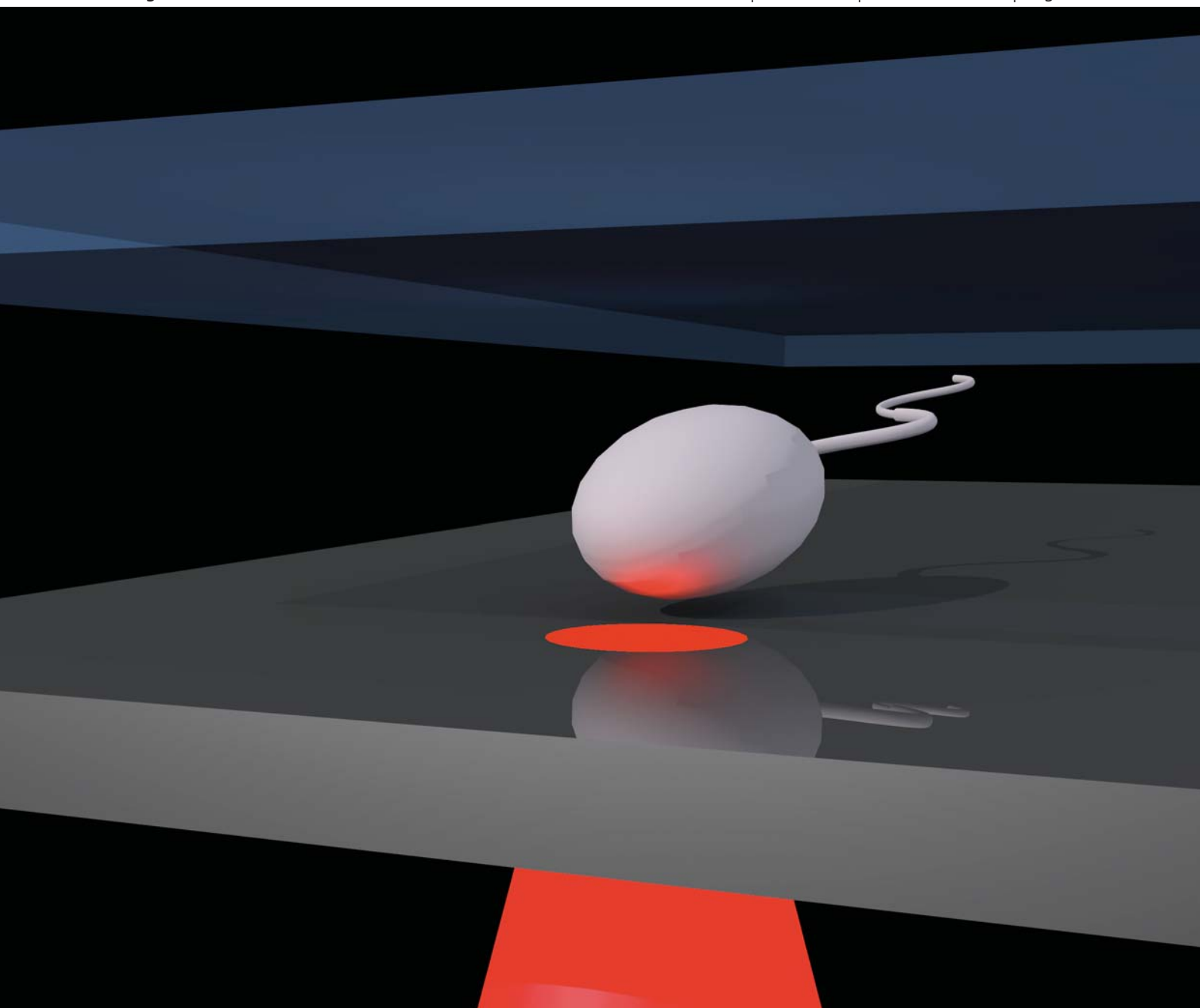


Lab on a Chip

Micro- & nano- fluidic research for chemistry, physics, biology, & bioengineering

www.rsc.org/loc

Volume 10 | Number 23 | 7 December 2010 | Pages 3185–3308



ISSN 1473-0197

RSC Publishing

PAPER

Ohta *et al.*

Motile and non-motile sperm diagnostic manipulation using optoelectronic tweezers

Motile and non-motile sperm diagnostic manipulation using optoelectronic tweezers

Aaron T. Ohta,^{†*a} Maurice Garcia,^{†^b} Justin K. Valley,^c Lia Banie,^b Hsan-Yin Hsu,^c Arash Jamshidi,^c Steven L. Neale,^c Tom Lue^b and Ming C. Wu^c

Received 4th June 2010, Accepted 12th August 2010

DOI: 10.1039/c0lc00072h

Optoelectronic tweezers was used to manipulate human spermatozoa to determine whether their response to OET predicts sperm viability among non-motile sperm. We review the electro-physical basis for how live and dead human spermatozoa respond to OET. The maximal velocity that non-motile spermatozoa could be induced to move by attraction or repulsion to a moving OET field was measured. Viable sperm are attracted to OET fields and can be induced to move at an average maximal velocity of $8.8 \pm 4.2 \mu\text{m s}^{-1}$, while non-viable sperm are repelled to OET, and are induced to move at an average maximal velocity of $-0.8 \pm 1.0 \mu\text{m s}^{-1}$. Manipulation of the sperm using OET does not appear to result in increased DNA fragmentation, making this a potential method by which to identify viable non-motile sperm for assisted reproductive technologies.

Introduction

Infertility, commonly defined as the inability to achieve pregnancy after 12 months of sexual relations without contraception,¹ affects around 15% of US couples in reproductive age. The male partner infertility is responsible for up to 50% of these cases.^{1,2} Common causes of male factor infertility are absence of sperm viability, low sperm count, and poor sperm function resulting in sperm inability to fertilize the oocyte naturally. A treatment option available to men with limited numbers of sperm and/or sperm of limited mobility or viability is intracytoplasmic sperm injection (ICSI).³ In this procedure, fertilization is achieved by injecting a single sperm directly into the oocyte (egg). Since the introduction of ICSI in 1992, this procedure has rapidly gained acceptance, and is used in 63% of US assisted reproductive procedures.⁴

A major concern related to ICSI is sperm selection: because which specific sperm ultimately fertilizes the oocyte is a matter of operator selection, the quality of the individual sperm selected is of paramount importance. Selection of non-viable sperm, for example, will result in the absence of fertilization, or an embryo that will ultimately be non-viable, thereby wasting a valuable oocyte. The selection of viable sperm for ICSI is challenging, and generally relies on the presence of sperm mobility to ensure that the sperm selected is actually viable.⁵ However, for patients who have limited, or even absent sperm motility (asthenospermia), selection of viable sperm on the basis of sperm motility can be virtually impossible. Reduced sperm motility is also often encountered in sperm samples that have been cryopreserved (frozen) before use. The freezing process invariably reduces mean

sperm motility, and can render specimens with poor baseline motility virtually immotile. Upon thawing of the sample, previously motile sperm can be rendered non-motile. While for many patients a sizable fraction of the sample may still be viable, the challenge is how to distinguish viable from non-viable sperm.

Current sperm viability assays are limited by subjectivity, sensitivity, and potential toxicity. The Trypan Blue dye exclusion test is a gold-standard cell viability assay, but its toxicity precludes subsequently using sperm exposed to Trypan Blue for ICSI. Another dye-based assay, eosin–nigrosin staining, involves an air-drying step which renders the tested sperm unavailable for further use.⁶ Ultimately, the current standard approach to sperm selection for use in ICSI procedures is based on the presence of motility, and, in the absence of this, sperm morphology.

We have previously reported that optoelectronic tweezers (OET) can non-invasively distinguish between live and dead cells and provide a means of sorting them using optically induced dielectrophoresis.⁷ Many different types of cells respond to the optically induced dielectrophoretic force, including red blood cells,⁸ white blood cells,^{7,9} HeLa cells,^{9–12} Jurkat cells,^{9,12} and oocytes.¹³ However, depending upon the electrical properties of the cell, the magnitude of the OET-induced force will vary. Previously, we demonstrated the separation of live and dead sperm.¹⁴ Here, the difference in OET force between viable and non-viable sperm is quantified, demonstrating that OET is capable of selecting viable *non-motile* sperm for use in ICSI procedures. In addition, it is shown that OET manipulation does not increase DNA fragmentation of the sperm under manipulation, which is an important concern if the sperm are to be used to create an embryo using assisted reproductive technologies.

Optically induced dielectrophoresis

Optoelectronic tweezers work by using optical patterns to control the electric field within a photosensitive device.⁷ Projected light, which can be from coherent or incoherent sources, reduces the impedance of a photosensitive layer, and creates regions of high electric field. The resulting electric field gradients

^aDepartment of Electrical Engineering, University of Hawaii at Manoa, Honolulu, HI, 96822, USA. E-mail: aohta@hawaii.edu; Fax: +1-808-956-3427; Tel: +1-808-956-8196

^bDepartment of Urology, University of California, San Francisco, CA, USA

^cDepartment of Electrical Engineering & Computer Sciences, University of California, Berkeley, CA, 94720, USA

[†] Contributed equally to this work.

give rise to a dielectrophoretic (DEP) force that can be used to manipulate micro- and nanoparticles.^{7,15,16} The induced DEP force on spherical particles is given by:

$$F_{\text{DEP}} = 2\pi r^3 \epsilon_m \text{Re}(\text{CM}) \text{grad}(E_{\text{rms}}^2), \quad (1)$$

where r is the particle radius, ϵ_m is the permittivity of the medium surrounding the particle, and E_{rms} is the root-mean-square electric field strength.¹⁷ The Clausius–Mossotti (CM) factor for a homogeneous spherical particle is given by:

$$\text{CM} = (\epsilon_p' - \epsilon_m') / (\epsilon_p' + 2\epsilon_m'), \quad (2)$$

where ϵ_p' and ϵ_m' are complex functions of the electrical properties of the cell and the surrounding media, respectively, and the frequency of the electric field.¹⁷ The general form of ϵ' is given by:

$$\epsilon' = \epsilon - j\sigma/\omega, \quad (3)$$

where ϵ and σ are the permittivity and conductivity of the cell or media, and ω is the frequency of the applied electric field.

The CM factor for mammalian cells needs to be altered, as they are not homogeneous throughout their volume. To simplify calculations, mammalian cells are typically approximated using a single-shell model that gives an effective permittivity that is an equivalent expression to eqn (3). The effective permittivity¹⁸ is given by:

$$\epsilon_p' = (rC_{\text{mem}}\epsilon_{\text{int}}') / (\epsilon_{\text{int}}' + rC_{\text{mem}}), \quad (4)$$

where ϵ_{int}' is the complex internal conductivity of the cell, and it is assumed that the thickness of the cell membrane, d , is much less than the radius of the cell interior, r . The membrane capacitance is given by:

$$C_{\text{mem}} = (\epsilon_{\text{mem}} - j\sigma_{\text{mem}}) / d. \quad (5)$$

In the case of cells, eqn (4) and (5) are used to solve eqn (3). The result of eqn (3) can then be used with eqn (1) and (2) to solve for the magnitude of the DEP force, which is used to predict the induced force on cells.

Live and dead cells in a low-conductivity isotonic media can have a large difference in induced DEP force, due to physiological changes in the cells. Live cells in an isotonic low-conductivity solution are able to maintain a higher ionic concentration in their interior as compared to the surrounding media. However, as the cell dies, the ion differential is no longer maintained, as the cell membrane becomes permeable to ions. Thus, the interior of a dead cell gains electrical properties that are more similar to the isotonic media. The simulated DEP force as a function of frequency for live and dead cells is shown in Fig. 1. The cell electrical parameters correspond to B cells, since this simulated behavior has been verified experimentally,⁷ but similar results can be expected for other cell types. The parameters used in the simulation are given in Table 1.

The normalized DEP forces for live cells (curve a) and dead cells (curve b) have different directions at a frequency of approximately 100 kHz. Live cells have a positive DEP force, indicating attraction to high electric field gradients, while the negative DEP force of the dead cells indicates repulsion from the

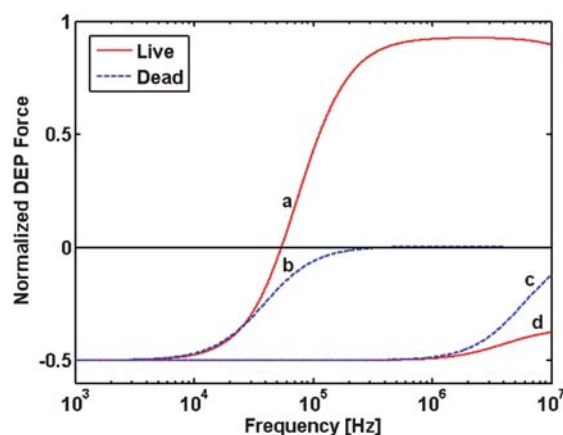


Fig. 1 Simulated normalized dielectrophoretic (DEP) force on live and dead cells. Curves a and b correspond to live and dead cells, respectively, in a 10 mS m^{-1} low-conductivity isotonic solution. Curves c and d correspond to live and dead cells, respectively, in a 1.5 S m^{-1} high-conductivity cell culture medium.

electric field gradients. This difference in polarity only occurs in low-conductivity solutions; if the media conductivity is increased to 1.5 S m^{-1} , typical of cell culture media, then live cells (curve c) and dead cells (curve d) are both repelled by the electric field gradients. Therefore, in order to maximize the differentiation between live and dead cells, it is desirable to use low-conductivity isotonic media at applied electric field frequencies near 100 kHz.

Materials and methods

Fabrication of optoelectronic tweezers device

OET devices were coated with a poly(ethylene glycol) (PEG) antifouling layer, according to a previous published fabrication process.²⁰ Briefly, the amorphous silicon electrode of a standard OET device⁷ is coated with a 10 nm thick layer of silicon dioxide using plasma-enhanced chemical vapor deposition. Subsequently, the silicon-dioxide-coated amorphous silicon electrodes are rinsed in a series of chemical washes, then a PEG-silane of 2-[methoxy(polyethyleneoxy)propyl]-trimethoxysilane (M_w 5000 obtained from Nektar) is melted onto the electrode surfaces. A similar process is used to coat the indium-tin-oxide electrode surfaces, although the silicon dioxide deposition step is omitted.

Sperm samples

Fresh ejaculate specimens from 4 healthy male volunteers were obtained in accordance with the policies of our institution's Committee on Human Research. All specimens were maintained at room temperature, and tested within six hours of production. Isotonic solution was prepared by adding 8.5% (w/v) sucrose and 0.3% (w/v) dextrose to deionized (DI) water. Trypan Blue powder (Sigma Aldrich) was added to DI water at a concentration of 0.4% (w/v) to create the Trypan solution for viability verification.

Table 1 Parameters for DEP force simulation

$\epsilon_m = 78 \cdot 8.85 \times 10^{-12} \text{ F m}^{-1}$	Permittivity of media
$\sigma_{m,\text{isotonic}} = 10 \text{ mS m}^{-1}$	Conductivity of low-conductivity isotonic solution
$\sigma_{m,\text{culture}} = 1.5 \text{ S m}^{-1}$	Conductivity of cell culture media
Live B cell parameters	
$\epsilon_{\text{int}} = 154.4 \cdot 8.85 \times 10^{-12} \text{ F m}^{-1}$	Permittivity of cell interior ¹⁹
$\sigma_{\text{int}} = 0.73 \text{ S m}^{-1}$	Conductivity of cell interior ¹⁹
$r = 3.29 \text{ }\mu\text{m}$	Cell radius ¹⁸
$C_{\text{mem}} = 0.0126 \text{ F m}^{-2}$	Cell membrane capacitance ¹⁹
Dead B cell parameters	
$\epsilon_{\text{int}} = 78 \cdot 8.85 \times 10^{-12} \text{ F m}^{-1}$	Permittivity of cell interior = media permittivity
$\sigma_{\text{int},\text{isotonic}} = 10 \text{ mS m}^{-1}$	Conductivity of cell interior = conductivity of isotonic solution
$\sigma_{\text{int},\text{culture}} = 1.5 \text{ S m}^{-1}$	Conductivity of cell interior = conductivity of culture media

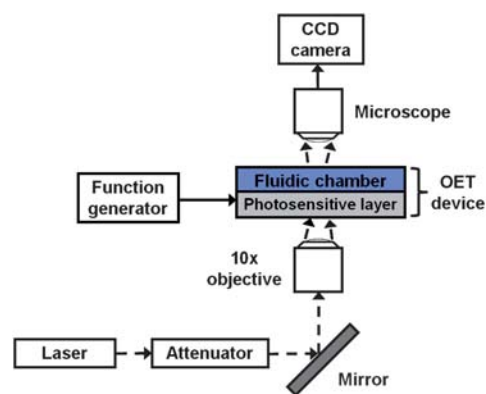
Comet assay

An alkaline comet assay (Trevigen, USA) was used to measure single and double-stranded DNA fragmentation in an unwashed diluted semen sample. Each subject's sample was divided into aliquots. Aliquots of sperm exposed and not exposed to OET assay conditions underwent COMET assay. In addition, we sought to determine whether isolated components of the OET assay independently caused DNA damage: exposure of sperm to the minimally conductive OET suspension medium, passage of sperm through the OET chip (with no exposure to OET energy), and, possible damage dose–response effect from OET energy parameters. Aliquots of each subject's semen sample were exposed to these various conditions, and then underwent COMET assay and image capture using fluorescence microscopy. Captured images were assessed using Cometsure™ analysis software to measure three assay criteria: percentage of DNA in tail, olive moment (product of the percentage of total DNA in the tail and the distance between the centers of the mass of head and tail regions), and tail moment (product of the tail length and the fraction of total DNA in the tail). All assays were performed in triplicate, and mean values are reported.

Five separate test samples were prepared from the subject's sample. The test samples consist of: (1) the fresh ejaculate sample (pure); (2) sperm suspended in a 1 : 100 dilution of the pure sample to isotonic solution, and flushed through the OET device (isotonic); (3) sperm in isotonic solution that are exposed to an applied bias of 10 V_{pp} at 100 kHz and an optical pattern at an intensity of 80 mW cm^{-2} for 30 s (low dose); (4) a sample similar to the low dose sample, except the applied bias is increased to 20 V_{pp} at 100 kHz (high dose); (5) pure sample that has been heated to $100 \text{ }^\circ\text{C}$ for 20 minutes in order to induce DNA damage, providing a positive control (heat).

Experimental setup and protocol

The fabricated PEG-coated OET devices were used to manipulate sperm samples. OET actuation was provided by a 10 mW, 635 nm diode laser, focused onto the OET surface using a 10× objective lens (Fig. 2). The output of the laser is attenuated, resulting in an intensity of 40 mW cm^{-2} incident upon the OET device. The laser is incident from the glass substrate underneath the photosensitive layer of the OET device. Thus, the sperm

**Fig. 2** Setup of the OET device for sperm manipulation.

sample is further screened from the actuation laser by the absorption of the light in the photosensitive layer.

Fresh ejaculate specimens were evaluated using OET. The adequacy of each specimen was confirmed by the presence of motile sperm in the sample. In order to confirm the viability of non-motile spermatozoa, a gold-standard viability reference assay was used: samples were mixed in a 1 : 1 volume ratio with 0.4% Trypan Blue dye in DI water, and incubated at room temperature for 3 minutes. The sperm/Trypan mixture was then diluted approximately 100 times by adding isotonic solution. The conductivity of the diluted sperm solution was adjusted to be 6.5 mS m^{-1} for all samples.

A $20 \text{ }\mu\text{L}$ aliquot of the Trypan-stained sperm sample was pipetted into the PEG-coated OET devices. Within 15 minutes of incubation of the sperm with Trypan Blue, 50 individual sperm were evaluated from each donor. As a positive control, five motile sperm were trapped using OET, verifying that a positive OET response was induced on these viable sperm. The OET-induced velocity of 25 non-motile sperm that excluded the Trypan Blue dye (confirms viability) was also evaluated. In addition, the OET-induced velocity of 20 dead (Trypan Blue stained) sperm was measured. All velocity measurements were done using an applied bias of 9 V_{pp} at 100 kHz. This voltage was empirically determined to provide an electric field strong enough for significant manipulation velocities (attractive velocities greater than $2 \text{ }\mu\text{m s}^{-1}$) while minimizing the electric field exposure of the sperm under manipulation.

Results and discussion

Sperm viability assay

A total of 200 individual spermatozoa from the 4 separate subjects were assayed. All (100%) of the motile sperm visualized in each specimen were Trypan Blue negative, and all of those assayed ($N = 25$) experienced positive OET. All (100%) sperm experiencing positive OET were Trypan Blue negative ($N = 100$). The Trypan-Blue-positive spermatozoa ($N = 80$) demonstrated either no response or a weak repulsive response to the OET manipulation pattern. Maximal OET-induced velocities of live and dead non-motile spermatozoa are shown in Fig. 3. The average velocity of live non-motile sperm in the OET device is $8.8 \pm 4.2 \text{ }\mu\text{m s}^{-1}$, averaged over 100 cells from 4 separate donors.

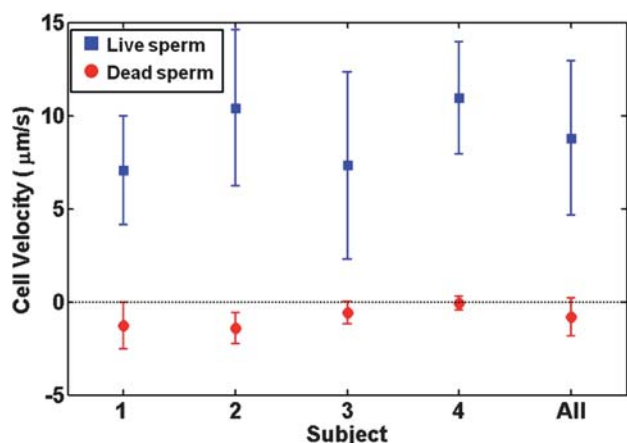


Fig. 3 OET-induced velocities of live non-motile sperm and dead sperm. The error bars indicate the standard deviation of the measurements. "All" refers to sperm velocities averaged across all 4 subjects.

The average velocity of dead sperm is $-0.8 \pm 1.0 \mu\text{m s}^{-1}$ with the negative value indicating a negative OET force. The dead Trypan-Blue-positive sperm exhibited some variability in their OET response, exhibiting either weak negative OET (60%) or no response to the OET pattern (40%). However, no Trypan-Blue-positive sperm exhibited a positive OET response. Thus, these results confirm that OET can distinguish among, and sort live non-motile spermatozoa from dead spermatozoa.

Thus, live spermatozoa that are either motile or non-motile experience a positive DEP force, which agrees with the results predicted by the DEP theory discussed earlier. Dead spermatozoa, as identified by Trypan Blue staining, experience either a negative DEP force or are unresponsive to manipulation, which also agrees with the DEP theory. Although further experiments are necessary to create an electrical model of live and dead spermatozoa, the trend of DEP force can be predicted using the known electrical parameters live and dead B cells. Similarly, this technique can be extended to the separation of other live and dead cells. The electrical properties of the live *versus* dead cells do not need to be measured in detail, as long as an electric field frequency that is suitable for the separation can be empirically determined (*e.g.* approximately 100 kHz for the cells in Fig. 1).

Characterization of induced DNA fragmentation

If OET sorting is to be used as a screening process for *in vitro* fertilization, it must be gentle enough to avoid inducing DNA damage on sperm. The effects of DEP force on live cells have been previously studied,^{21–23} and shown to be minimally invasive, even for cells subjected to DEP manipulation in low-conductivity isotonic solution.²⁴ However, previous studies did not measure DNA damage in the cells under manipulation, which is of concern for any assisted reproductive technology. Thus, the DNA fragmentation of sperm manipulated using OET was quantified using a standard single-cell gel electrophoresis assay, the comet assay.²⁵

A PEG-coated OET device with a microfluidic chamber was used in the comet assay experiments. The microfluidic chamber measures $1 \text{ cm} \times 1 \text{ cm} \times 100 \mu\text{m}$, and allows the introduction and removal of the test samples using syringe pumps. A fresh

ejaculate specimen from one subject was used for the alkaline comet assay²⁶ (pH 10, Trevigen, USA), and subdivided into five separate test samples, as mentioned in the Materials and methods section.

The pure sample serves as a negative control for the assay, and the isotonic sample serves as a negative control for the experimental samples, which are all diluted using low-conductivity isotonic buffer. The low-dose sample represents the energy exposure during a typical OET sorting experiment, whereas the high-dose sample is exposed to twice the typical electric field strength. It was expected that the electric field would be the main factor in causing damage to the cells, as the intensity of the optical patterns are orders of magnitude lower than intensities which can cause photodamage.^{27,28} Finally, the heat sample serves as a positive control for the assay.

The results of the comet assay are quantified according to percentage of DNA in the "tail," which measures the amount of DNA fragmentation, and the tail moment. The tail moment is a measure of the separation between the intensity-weighted center of the "head" of a cell and the intensity-weighted "tail" of a cell. Longer tail moments are indicative of more DNA damage. A minimum of 200 cells per slide per assay were measured. One-way ANOVA and overall *F*-tests (two-tail α , significance at 0.05, 95% CI) were performed on the mean percentage of DNA in tail and the tail moment in each subject's pure, isotonic, low-dose, and high-dose samples. The heat-treated samples were excluded from the regression analysis, as it was a positive control.

The one-way ANOVA (two-tailed α , significance = $p < 0.05$) detected no significant increase in percentage of DNA in the tail (Fig. 4) or tail moments (Fig. 5) between the pure, isotonic, low-dose, and high-dose samples. In addition, the heat-treated sample had greater DNA fragmentation as compared to the other samples. The overall *F*-test also showed no difference in DNA fragmentation among the isotonic samples and the samples exposed to both a low and high dose of OET energy. Thus, OET manipulation should provide viable cells for *in vitro* fertilization after sorting operations are performed.

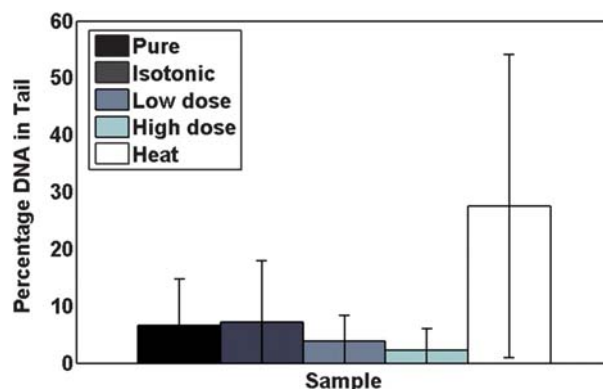


Fig. 4 DNA damage in OET-manipulated sperm as indicated by the percentage of DNA in the tail, determined using the comet assay. For each subject, similar amounts of DNA fragmentation are evident in the pure and isotonic samples, as well as the samples manipulated using OET (low dose and high dose). More DNA fragmentation is present in sperm that was heated to 100 °C for 20 minutes ("heat" sample).

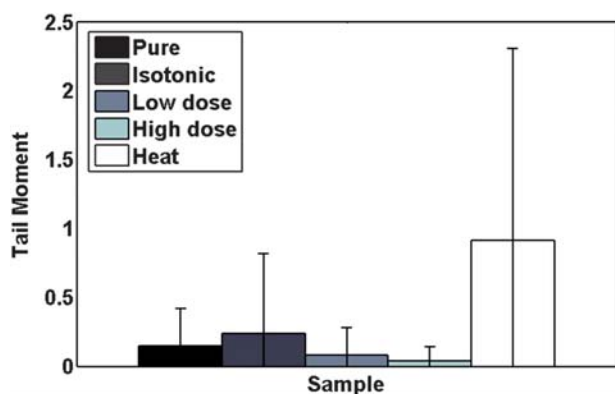


Fig. 5 DNA damage in OET-manipulated sperm as indicated by the tail moment, determined using the comet assay. The cells under test correspond to the same cells as the results in Fig. 4. For each subject, similar amounts of DNA fragmentation are present in the pure and isotonic samples, as well as the samples manipulated using OET. More DNA damage is present in sperm that was heated to 100 °C for 20 minutes ("heat" sample).

Conclusions

We have demonstrated that OET is capable of non-invasively identifying, assessing, and sorting viable live non-motile sperm from non-viable sperm, without introducing DNA damage on the cells under manipulation. However, the experiments presented here were performed with fresh unwashed semen. Sperm washing procedures, which commonly include centrifugation through a density gradient, may contribute to sperm damage by removing antioxidant-rich seminal plasma, and, possibly by induction of oxidative stress and formation of free-radicals/reactive oxygen species (ROS).^{29,30} The compatibility of the OET assay with unwashed samples suggest that it is possible to forgo typical sperm-washing protocols when using fresh samples.

On the other hand, centrifugation removes the antioxidant-rich seminal plasma and increases ROS production and release, both in sperm and in leukocytes.²⁹ Activation of leukocytes by centrifugation may increase ROS production up to 100-fold.³⁰

In addition, an optimized microfluidic setup is currently being integrated with the PEG-coated OET devices to enable more efficient sample retrieval of the sorted cells.

Acknowledgements

This project was funded in part by the National Institutes of Health (NIH) through the Center for Cell Control, grant number PN2 EY018228. A. Ohta and M. Garcia would like to thank G. Lin for technical assistance, the UCSF Knuppe Molecular Urology Lab where key portions of this work were performed, and the UC Berkeley Microlab, where all devices were fabricated. M. Garcia thank D. J. Lamb, R. Yanagimachi, S. Moisyadi, and F. Marchetti for helpful discussion. M. Garcia would like to acknowledge funding and publication support from NIH/NCRR UCSF-CTSI Grant Number UL1 RR024131, and NIH K-12 Men's Reproductive Health Research (MRHR) Grant. Care and handling of all subject information, specimens, and

data associated with this work was in accordance with University of California San Francisco's Committee on Human Research policies.

References

- D. J. Lamb and L. I. Lipshultz, *Curr. Opin. Neurol.*, 2000, **10**, 359–362.
- S. Oehninger, *J. Androl.*, 2000, **21**, 814–821.
- G. Palermo, H. Joris, P. Devroey and A. Vansteirteghem, *Lancet*, 1992, **340**, 17–18.
- US Department of Health and Human Services and Centers for Disease Control and Prevention, Assisted Reproductive Technology (ART) Report: National Summary, 2007, <http://apps.nccd.cdc.gov/ART/NSR.aspx?SelectedYear=2007>.
- B. S. Cho, T. G. Schuster, X. Zhu, D. Chang, G. D. Smith and S. Takayama, *Anal. Chem.*, 2003, **75**, 1671–1675.
- L. Bjorndahl, I. Soderlund and U. Kvist, *Hum. Reprod.*, 2003, **18**, 813–816.
- P. Chiou, A. T. Ohta and M. C. Wu, *Nature*, 2005, **436**, 370–372.
- A. T. Ohta, P. Chiou, T. H. Han, J. C. Liao, U. Bhardwaj, E. R. B. McCabe, F. Yu, R. Sun and M. C. Wu, *J. Microelectromech. Syst.*, 2007, **16**, 491–499.
- A. T. Ohta, P. Chiou, H. L. Phan, S. W. Sherwood, J. M. Yang, A. N. K. Lau, H. Hsu, A. Jamshidi and M. C. Wu, *IEEE J. Sel. Top. Quantum Electron.*, 2007, **13**, 235–243.
- J. K. Valley, S. Neale, H. Hsu, A. T. Ohta, A. Jamshidi and M. C. Wu, *Lab Chip*, 2009, **9**, 1714–1720.
- S. L. Neale, A. T. Ohta, H. Hsu, J. K. Valley, A. Jamshidi and M. C. Wu, *Opt. Express*, 2009, **17**, 5232–5239.
- H. Hsu, A. T. Ohta, P. Chiou, A. Jamshidi, S. L. Neale and M. C. Wu, *Lab Chip*, 2010, **10**, 165–172.
- H. Hwang, D. Lee, W. Choi and J. Park, *Biomicrofluidics*, 2009, **3**, 014103–014110.
- M. Garcia, A. T. Ohta, T. J. Walsh, E. Vittinghof, G. Lin, M. C. Wu and T. F. Lue, *J. Urol. (N. Y., N.Y., U. S.)*, Dec. 2010, in press.
- M. Tien, A. T. Ohta, K. Yu, S. L. Neale and M. C. Wu, *Appl. Phys. A: Mater. Sci. Process.*, 2009, **95**, 967–972.
- A. Jamshidi, P. J. Pauzaskie, P. J. Schuck, A. T. Ohta, P. Chiou, J. Chou, P. Yang and M. C. Wu, *Nat. Photonics*, 2008, **2**, 85–89.
- T. B. Jones, *Electromechanics of Particles*, Cambridge University Press, Cambridge, 1995.
- P. R. C. Gascoyne, F. F. Becker and X. B. Wang, *Bioelectrochem. Bioenerg.*, 1995, **36**, 115–125.
- J. Yang, Y. Huang, X. Wang, X. Wang, F. F. Becker and P. R. C. Gascoyne, *Biophys. J.*, 1999, **76**, 3307–3314.
- A. N. K. Lau, A. T. Ohta, H. L. Phan, H. Hsu, A. Jamshidi, P. Chiou and M. C. Wu, *Lab Chip*, 2009, **9**, 2952–2957.
- A. Docolis, N. Kalogerakis and L. A. Behie, *Cytotechnology*, 1999, **30**, 133–142.
- G. Fuhr, T. Muller, V. Baukloh and K. Lucas, *Hum. Reprod.*, 1998, **13**, 136–141.
- S. Dessie, F. Rings, M. Holker, M. Gilles, D. Jennen, E. Tholen, V. Havlicek, U. Besenfelder, V. L. Sukhorukov, U. Zimmermann, J. M. Endter, M. Sirard, K. Schellander and D. Tesfaye, *Reproduction*, 2007, **133**, 931–946.
- C. T. Ho, R. Z. Lin, W. Y. Chang, H. Y. Chang and C. H. Liu, *Lab Chip*, 2006, **6**, 724–734.
- D. W. Fairbairn, P. L. Olive and K. L. O'Neill, *Mutat. Res., Rev. Genet. Toxicol.*, 1995, **339**, 37–59.
- R. R. Tice, P. W. Andrews and N. P. Singh, *Basic Life Sci.*, 1990, **53**, 291–301.
- K. Konig, H. Liang, M. W. Berns and B. J. Tromberg, *Nature*, 1995, **377**, 20–21.
- S. K. Mohanty, A. Rapp, S. Monajembashi, P. K. Gupta and K. O. Greulich, *Radiat. Res.*, 2002, **157**, 378–385.
- R. J. Aitken and J. S. Clarkson, *J. Androl.*, 1988, **9**, 367–376.
- W. C. L. Ford, in *Clinical IVF Forum: Current Views in Assisted Reproduction*, ed. P. L. Matson and B. A. Liebermann, University Press, Manchester, 1990, pp. 123–139.